

## Fitting net photosynthetic light-response curves with *Microsoft Excel* – a critical look at the models

F. de A. LOBO<sup>\*,+</sup>, M.P. de BARROS<sup>\*\*</sup>, H.J. DALMAGRO<sup>\*\*</sup>, Â.C. DALMOLIN<sup>\*\*</sup>, W.E. PEREIRA<sup>\*\*\*</sup>,  
É.C. de SOUZA<sup>#</sup>, G.L. VOURLITIS<sup>###</sup>, and C.E. RODRÍGUEZ ORTÍZ<sup>###</sup>

*Departamento de Solos e Engenharia Rural, FAMEV/UFMT, 78060-900, Cuiabá-MT, Brasil\**

*Programa de Pós-Graduação em Física Ambiental, IF/UFMT, 78060-900, Cuiabá-MT, Brasil\*\**

*Departamento de Ciências Fundamentais e Sociais, CCA/UFPA, 58397-000, Areia-PB, Brasil\*\*\**

*Departamento de Estatística, ICET/UFMT, 78060-900, Cuiabá-MT, Brasil#*

*Department of Biological Science, CSUSM, San Marcos-CA, 92096-0001, USA###*

*Departamento de Botânica e Ecologia, IB/UFMT, 78060-900, Cuiabá-MT, Brasil###*

### Abstract

In this study, we presented the most commonly employed net photosynthetic light-response curves ( $P_N/I$  curves) fitted by the Solver function of *Microsoft Excel*. *Excel* is attractive not only due to its wide availability as a part of the *Microsoft Office* suite but also due to the increased level of familiarity of undergraduate students with this tool as opposed to other statistical packages. In this study, we explored the use of *Excel* as a didactic tool which was built upon a previously published paper presenting an *Excel* Solver tool for calculation of a net photosynthetic/chloroplastic  $\text{CO}_2$ -response curve. Using the *Excel* spreadsheets accompanying this paper, researchers and students can quickly and easily choose the best fitted  $P_N/I$  curve, selecting it by the minimal value of the sum of the squares of the errors. We also criticized the misuse of the asymptotic estimate of the maximum gross photosynthetic rate, the light saturation point estimated at a specific percentile of maximum net photosynthetic rate, and the quantum yield at zero photosynthetic photon flux density and we proposed the replacement of these variables by others more directly linked to plant ecophysiology.

*Additional key words:* curve fitting; iteration; nonlinear regression;  $P_N/I$  curve; Solver function.

### Introduction

The net photosynthetic light-response curve ( $P_N/I$  curve) describes the net  $\text{CO}_2$  assimilation by a plant leaf ( $P_N$ ) as a function of an increase in the photosynthetic photon flux density ( $I$ ) from the total absence of light to a high

level of light, e.g.  $2,000 \mu\text{mol}(\text{photon}) \text{m}^{-2} \text{s}^{-1}$ .

The curve presents several phases. At the beginning, from complete darkness to the light compensation point ( $I_{\text{comp}}$ ), there is a rapid increase in  $P_N$  with  $I$ , due to the

Received 17 April 2012, accepted 17 January 2013.

<sup>+</sup>Corresponding author; e-mail: f\_a\_lobo@ufmt.br

*Abbreviations:* ARE – average relative errors;  $C_c$  – chloroplast  $\text{CO}_2$  concentration;  $C_i$  – intercellular  $\text{CO}_2$  concentration;  $I$  – photosynthetic photon flux density;  $I_{\text{comp}}$  – light compensation point;  $I_{\text{max}}$  – light saturation point beyond which there is no significant change in  $P_N$ ;  $I_{\text{sat}}$  – light saturation point;  $I_{\text{sat}(n)}$  – light saturation point at a specific percentile ( $n$ ) of  $P_{N\text{max}}$ ;  $I_{\text{sat}(85)}$  – light saturation point for  $P_N + R_D$  equal to 85% of  $P_{N\text{max}}$ ;  $I_{\text{sat}(90)}$  – light saturation point for  $P_N + R_D$  equal to 90% of  $P_{N\text{max}}$ ;  $I_{\text{sat}(95)}$  – light saturation point for  $P_N + R_D$  equal to 95% of  $P_{N\text{max}}$ ;  $I_{(50)}$  – light saturation point for  $P_N + R_D$  equal to 50% of  $P_{N\text{max}}$ ;  $k$  – adjusting factor;  $P_g$  – gross photosynthetic rate;  $P_{g\text{max}}$  – maximum gross photosynthetic rate;  $P_N$  – net photosynthetic rate;  $P_{N(I\text{max})}$  – maximum net photosynthetic rate obtained at  $I = I_{\text{max}}$ ;  $P_{N\text{max}}$  – maximum net photosynthetic rate;  $R_D$  – dark respiration;  $R^2$  – coefficient of determination; SAE – sum of the absolute errors; SSE – sum of the squares of the errors;  $V_{\text{max}}$  – enzyme maximum velocity;  $\beta$  – adjusting factor;  $\gamma$  – adjusting factor;  $\theta$  – convexity factor;  $\phi$  – quantum yield;  $\phi(I)$  – quantum yield at a particular value of  $I$ ;  $\phi(I_{\text{comp}})$  – quantum yield at  $I = I_{\text{comp}}$ ;  $\phi(I_{\text{comp}} - I_{200})$  – quantum yield at the range between  $I_{\text{comp}}$  and  $I = 200 \mu\text{mol}(\text{photon}) \text{m}^{-2} \text{s}^{-1}$ ;  $\phi(I_0)$  – quantum yield at  $I = 0 \mu\text{mol}(\text{photon}) \text{m}^{-2} \text{s}^{-1}$ ;  $\phi(I_0 - I_{\text{comp}})$  – quantum yield at the range between  $I = 0 \mu\text{mol}(\text{photon}) \text{m}^{-2} \text{s}^{-1}$  and  $I_{\text{comp}}$ ;  $\phi_{\text{max}}$  – theoretical maximum quantum yield;  $\chi^2$  – Chi-square test.

*Acknowledgments:* This study was supported by grants from the Instituto Nacional de Ciência e Tecnologia em Áreas Úmidas (INAU), Programa Institutos Nacionais de Ciência e Tecnologia (CNPq/MCT), and from Fundação de Amparo à Pesquisa do Estado de Mato Grosso (FAPEMAT) and scholarships from Conselho Nacional de Desenvolvimento Científico e Tecnológico (CNPq). We would like to thank Dr. Clóvis Nobre de Miranda for allowing us to conduct the research on his farm and for giving us the facilities to work there.

natural decrease in dark respiration ( $R_D$ ), named the Kok effect (Kok 1949). The light compensation point is the value of  $I$  at which the  $\text{CO}_2$  assimilated by photosynthesis is in balance with the  $\text{CO}_2$  produced by light respiration and photorespiration, resulting in  $P_N$  equal to zero. Beyond this point, a supposed linear response of  $P_N$  to  $I$  can be seen until  $I$  reaches approximately  $200 \mu\text{mol}(\text{photon}) \text{m}^{-2} \text{s}^{-1}$ . This linear portion is the range that many authors use to calculate the “maximum quantum yield” ( $\phi_{(I_{\text{comp}} - I_{200})}$ ), which is the slope in that range, and beyond this range there is a region of nonlinear die-off before  $P_N$  reaches a semiplateau, where an increase in  $I$  does not provoke a proportional increase in  $P_N$  (Long and Hällgren 1993). The progressive curvature in the ratio  $\delta P_N / \delta I$  in this region can be described by a convexity factor ( $\theta$ ) (Ögren 1993). Sometimes, after reaching the maximum value of  $P_N$ , a subsequent decrease in  $P_N$  with  $I$ , referred to as photoinhibition, can be observed (Ye 2007). Extensive literature is available describing the different phases of the curve and the effects of temperature,  $\text{CO}_2$  concentration, pH, chemical inhibitors of photosynthesis, and other factors (Long and Hällgren 1993, Govindjee *et al.* 2005, Zeinalov 2005, Lambers *et al.* 2008).

Many mathematical models may be used to describe  $P_N/I$  curves. Various parameters and variables calculated from these models are used to describe the photosynthetic capacity, efficiency, and other aspects. Those variables include  $I_{\text{comp}}$ , the asymptotic estimate of the maximum gross photosynthetic rate ( $P_{\text{gmax}}$ ), the light saturation point for  $P_N + R_D$  equal to 50% of maximum net photosynthetic rate ( $P_{N\text{max}}$ ) ( $I_{(50)}$ ), the light saturation point for  $P_N$  equal to a percentile of the  $P_{N\text{max}}$  ( $I_{\text{sat}(n)}$ ), the light saturation point ( $I_{\text{sat}}$ ), the quantum yield at  $I = 0 \mu\text{mol}(\text{photon}) \text{m}^{-2} \text{s}^{-1}$  ( $\phi_{(I_0)}$ ), the quantum yield obtained in the range between  $I_0$  and  $I_{\text{comp}}$  ( $\phi_{(I_0 - I_{\text{comp}})}$ ),  $\phi_{(I_{\text{comp}} - I_{200})}$ ,  $\phi$  obtained at any value of  $I$  ( $\phi_{(I)}$ ),  $\theta$ , and  $R_D$ .

Certain models are modifications of the originals, but sometimes these modifications produce serious problems that are not handled properly or, at best, they produce meaningless information. Kaipainen (2009) uses a modified Michaelis-Menten model (Eq. 2), assuming that  $I_{(50)}$  is the value of  $I$ , when  $P_N$  is equal to 50% of  $P_{\text{gmax}}$ ; however, that assumption is only true if the gross photosynthetic rate ( $P_g$ , which is equal to  $P_N + R_D$ ) is equal to 50% of  $P_{\text{gmax}}$ . A nonrectangular hyperbola, in its original form (Eq. 6), was modified by Chen *et al.* (2008) to give the form of Eq. 7, which produces misleading information about the value of  $P_N$  in the absence of light ( $I = 0$ ). In that case, when  $I = 0$ , it is expected that  $P_N = -R_D$ , but the modified model produces a value of  $P_N = \frac{P_{\text{gmax}}}{2\theta} - R_D$ . The original, exponential model (Eq. 8)

has many different variations. One of these variations can be seen in the papers of Lootens *et al.* (2004) and Devacht

*et al.* (2009), shown in Eq. 10, where it can be observed that  $P_N = -R_D$ , when  $I = I_{\text{comp}}$ , not when  $I = 0$ .

For the majority of  $P_N/I$  curves,  $P_{\text{gmax}}$  and  $I_{\text{sat}(n)}$  have a mathematical definition but they do not often have the desired ecophysiological meaning, resulting in frequent misuse by researchers if not applied with caution. Presenting the definition of  $P_{\text{gmax}}$  as the light-saturated rate of  $\text{CO}_2$  uptake is akin to defining it as “the point beyond which there is no significant change in  $P_N$ ”, which is not the case, because  $P_{\text{gmax}}$  is obtained when  $I$  is infinite. In other words,  $P_{\text{gmax}}$  is an abstraction, which forces the existence of  $I_{\text{sat}(n)}$ , which is by deduction also an abstraction. The same issues occur with the quantum yield ( $\phi$ ), which, given the variety of methods used for the calculation of this parameter, often serves more aptly as a source of doubt than as an explanatory variable.

Ye (2007) proposed a modified rectangular hyperbola model able to fit the photoinhibition stage and to estimate  $P_{\text{gmax}}$  and  $I_{\text{sat}}$ . The author also employs 4 different forms of  $\phi$ :  $\phi_{(I_0)}$ ,  $\phi_{(I_{\text{comp}})}$ ,  $\phi_{(I_0 - I_{\text{comp}})}$ , and  $\phi_{(I)}$ . Although this model has several advantages in relation to the previous  $P_N/I$  curves, the values of  $P_{\text{gmax}}$  and  $I_{\text{sat}}$  produced are occasionally out of the expected range of ecophysiological meaning, thereby failing to resolve a key issue observed in other models calculating  $P_{\text{gmax}}$  and  $I_{\text{sat}(n)}$ .

Because the mathematical models describing the  $P_N/I$  curve are nonlinear, there are several problems that must be taken into account when fitting a regression curve. Researchers must have good statistical and mathematical knowledge and moderately advanced skill using statistical programs, which may not be available for students and at times researchers. *Microsoft Excel* can offer a good alternative in this case, not only in terms of fitting the regression curve but also affording the opportunity for the users to see and understand the use of each equation employed in the calculations (Brown 2001). Particularly in developing countries, an important consideration is that there are no additional expenses beyond the *Microsoft Office* package required to calculate  $P_N/I$  curves. There are many routines in *Microsoft Excel*, which were developed taking this philosophy into account. Examples include several exercises in ecology and evolution (Donovan and Welden 2002), resampling for the mean and the calculation of its confidence interval (Christie 2004), a tool for classical plant growth analysis (Hunt *et al.* 2002), and more appropriate for this work, a step-by-step tool to fit nonlinear regression (Brown 2001).

The net photosynthetic/chloroplastic  $\text{CO}_2$  response curve ( $P_N/C_c$  curve) and the  $P_N/I$  curve are useful tools in plant physiology. Both curves assist researchers in understanding the effects of changes in one or more primary factors affecting photosynthesis. These models are also employed as a single leaf component of more complex models of entire plants or ecosystems (Harley and Baldocchi 1995, Lloyd *et al.* 1995).

Sharkey *et al.* (2007) developed an *Excel* routine to fit

net photosynthetic/intercellular CO<sub>2</sub> response ( $P_N/C_i$ ) or  $P_N/C_c$  curve, but until now, no *Excel* routine has been developed to fit  $P_N/I$  curves. In this study, we presented the most common mathematical models for fitting  $P_N/I$  curves adjusted by the Solver function of *Microsoft Excel*. We proposed a new approach to find the maximum value of  $I$  ( $I_{\max}$ ) that saturates  $P_N$ , considering it as the point

beyond which there is no significant change in  $P_N$ . For our applications,  $I_{\max}$  and the maximum value of  $P_N$  obtained at  $I = I_{\max}$  ( $P_{N(I_{\max})}$ ) are more appropriate than  $I_{\text{sat}}$  or  $I_{\text{sat}(n)}$  and  $P_{\text{gmax}}$ , due to their realistic magnitudes that give them their intended ecophysiological meaning. Likewise,  $\phi_{(I)}$  can provide much more information than all of the other calculations of  $\phi$ .

## Materials and methods

**Primary data:** Measurements were conducted on *Vochysia divergens* Pohl (Vochysiaceae) in a fragment of savanna ecosystem (Cerrado *stricto sensu*) located in Cuiabá, Mato Grosso, Brazil (15°43' S, 56°04' W).

A unique, disease free, mature leaf exposed to full sunlight was measured with a portable photosynthetic system (*LI-6400*, *LI-COR, Inc.*, Logan, NE, USA) coupled with a standard red/blue LED broadleaf cuvette (*6400-02B*, *LI-COR, Inc.*, Logan, NE, USA) and a CO<sub>2</sub> mixer (*6400-01*, *LI-COR, Inc.*, Logan, NE, USA). The measurements were obtained with a block temperature of 28°C, 50 to 60% relative humidity, and 400  $\mu\text{mol}(\text{CO}_2)$   $\text{mol}(\text{air})^{-1}$  of CO<sub>2</sub> concentration inside the chamber.

The  $P_N/I$  curve was performed using the autoprogram function. In this case, we chose the sequence of desired light settings of 2,000; 1,500; 1,250; 1,000; 800; 500; 250; 100; 50; 25, and 0  $\mu\text{mol}(\text{photon}) \text{m}^{-2} \text{s}^{-1}$ , a minimum wait time of 120 s, a maximum wait time of 200 s, and matching the infrared gas analyzers for 50  $\mu\text{mol}(\text{CO}_2)$   $\text{mol}(\text{air})^{-1}$  difference in the CO<sub>2</sub> concentration between the sample and the reference, which allowed them to be matched before every change in  $I$ . The measurement results are shown in Table 1.

**Mathematical models for  $P_N/I$  curves:** In this section, we presented the models that were the most frequently employed to fit  $P_N/I$  curves: the rectangular hyperbola Michaelis-Menten based models (Eqs. 1–3), the hyperbolic tangent based models (Eqs. 4,5), the nonrectangular

Table 1. Original data obtained from the net photosynthetic light-response curves of *V. divergens*.

| $I$ [ $\mu\text{mol}(\text{photon}) \text{m}^{-2} \text{s}^{-1}$ ] | $P_N$ [ $\mu\text{mol}(\text{CO}_2) \text{m}^{-2} \text{s}^{-1}$ ] |
|--|--|
| 0  | -1.55  |
| 25   | 0.06   |
| 50   | 1.60   |
| 100  | 4.10   |
| 250  | 8.74   |
| 500  | 12.00  |
| 800  | 13.60  |
| 1,000  | 14.30  |
| 1,250  | 14.80  |
| 1,500  | 15.00  |
| 2,000  | 15.50  |

hyperbola-based models (Eqs. 6,7), the exponential based models (Eqs. 8–10), and the Ye model (Eq. 11). All these mathematical models are well described in the literature (Baly 1935, Smith 1936, Webb *et al.* 1974, Jassby and Platt 1976, Prioul and Chartier 1977, Gallegos and Platt 1981, Prado *et al.* 1994, Prado and de Moraes 1997, Vervuren *et al.* 1999, Lootens *et al.* 2004, Ye 2007, Chen *et al.* 2008, Abe *et al.* 2009, Kaipiainen 2009).

We developed individual *Excel* routines for all of these models except for Eqs. 7 and 10 due to the previous comments about their performance.

$$P_N = \frac{\phi_{(I_0)} \times I \times P_{\text{gmax}}}{\phi_{(I_0)} \times I + P_{\text{gmax}}} - R_D \quad (1)$$

$$P_N = \frac{I \times P_{\text{gmax}}}{I + I_{(50)}} - R_D \quad (2)$$

$$P_N = \frac{\phi_{(I_0)} \times I \times P_{\text{gmax}}}{\sqrt{\phi_{(I_0)}^2 \times I^2 + P_{\text{gmax}}^2}} - R_D \quad (3)$$

$$P_N = P_{\text{gmax}} \times \tanh\left(\frac{\phi_{(I_0)} \times I}{P_{\text{gmax}}}\right) - R_D \quad (4)$$

$$P_N = P_{\text{gmax}} \times \tanh\left(\frac{I}{I_{\text{sat}}}\right) - R_D \quad (5) \quad P_N = \frac{\phi_{(I_0)} \times I + P_{\text{gmax}} - \sqrt{(\phi_{(I_0)} \times I + P_{\text{gmax}})^2 - 4\theta \times \phi_{(I_0)} \times I \times P_{\text{gmax}}}}{2\theta} - R_D \quad (6)$$

$$P_N = \frac{\phi_{(I_0)} \times I + \sqrt{(\phi_{(I_0)} \times I + P_{\text{gmax}})^2 - 4\theta \times \phi_{(I_0)} \times I \times P_{\text{gmax}}}}{2\theta} - R_D \quad (7) \quad P_N = \left\{ P_{\text{gmax}} \left[ 1 - \exp\left(\frac{-\phi_{(I_0)} \times I}{P_{\text{gmax}}}\right) \right] \right\} - R_D \quad (8)$$

$$P_N = \left\{ P_{\text{gmax}} \left[ 1 - \exp(-k(I - I_{\text{comp}})) \right] \right\} - R_D \quad (9)$$

$$P_N = \phi_{(I_0 - I_{\text{comp}})} \times \frac{1 - \beta \times I}{1 + \gamma \times I} \times (I - I_{\text{comp}}) \quad (11)$$

where:  $I$  – the photosynthetic photon flux density [ $\mu\text{mol}$  (photon)  $\text{m}^{-2} \text{s}^{-1}$ ];  $I_{\text{comp}}$  – the light compensation point [ $\mu\text{mol}$ (photon)  $\text{m}^{-2} \text{s}^{-1}$ ];  $I_{\text{sat}}$  – the light saturation point [ $\mu\text{mol}$ (photon)  $\text{m}^{-2} \text{s}^{-1}$ ];  $I_{(50)}$  – the light saturation point at  $P_N + R_D = 50\%$  of  $P_{\text{gmax}}$ ;  $k$  – an adjusting factor [ $\text{s} \text{m}^2 \mu\text{mol}(\text{photon})^{-1}$ ];  $P_{\text{gmax}}$  – the asymptotic estimate of the maximum gross photosynthetic rate [ $\mu\text{mol}(\text{CO}_2) \text{m}^{-2} \text{s}^{-1}$ ];  $P_N$  – the net photosynthetic rate [ $\mu\text{mol}(\text{CO}_2) \text{m}^{-2} \text{s}^{-1}$ ];  $R_D$  – the dark respiration rate [ $\mu\text{mol}(\text{CO}_2) \text{m}^{-2} \text{s}^{-1}$ ];  $\beta$  – an adjusting factor (dimensionless);  $\gamma$  – an adjusting factor (dimensionless);  $\theta$  – the convexity (dimensionless);  $\phi_{(I_0)}$  – the quantum yield at  $I = 0$  [ $\mu\text{mol}(\text{CO}_2) \mu\text{mol}$  (photon) $^{-1}$ ];  $\phi_{(I_0 - I_{\text{comp}})}$  – the quantum yield obtained at the range between  $I_0$  and  $I_{\text{comp}}$  [ $\mu\text{mol}(\text{CO}_2) \mu\text{mol}(\text{photon})^{-1}$ ].

**Calculated variables:** All variables and regression parameters used to analyze the  $P_N/I$  curves were calculated or taken from each model, respectively.

$P_{\text{gmax}}$ ,  $R_D$ , and  $I_{\text{sat}}$  were not any of the parameters in Eq. 11. Instead, they are calculated using Eqs. 12–14, respectively (Ye 2007).

$$P_{\text{gmax}} = \phi_{(I_0 - I_{\text{comp}})} \times \frac{1 - \beta \times I_{\text{sat}}}{1 + \gamma \times I_{\text{sat}}} \times (I_{\text{sat}} - I_{\text{comp}}) + R_D \quad (12)$$

$$R_D = \phi_{(I_0 - I_{\text{comp}})} \times I_{\text{comp}} \quad (13)$$

$$I_{\text{sat}} = \frac{\sqrt{(\beta + \gamma) \times (1 + \gamma \times I_{\text{comp}})}}{\gamma} \quad (14)$$

As  $\phi_{(I_0)}$  is one of the parameters only in Eqs. 1, 3, 4, 6–8, and 10, for the other equations it was calculated as the derivative of these models at  $I = 0$ . For any value of  $I$ , the general  $\phi_{(I)}$  is calculated as the derivative of the  $P_N/I$  curve with respect to  $I$ . The corresponding derivative equations for the mathematical models employed in this study to develop individual *Excel* routines (Eqs. 1–6, 8, 9, and 11) are presented in Eqs. 15–20, 21, 22, and 23, respectively.

$$\phi_{(I)} = \frac{\phi_{(I_0)} \times P_{\text{gmax}}^2}{(\phi_{(I_0)} \times I + P_{\text{gmax}})^2} \quad (15)$$

$$\phi_{(I)} = \frac{I_{(50)} \times P_{\text{gmax}}}{(I + I_{\text{sat}(50)})^2} \quad (16)$$

$$P_N = P_{\text{gmax}} \left\{ 1 - \exp \left[ -\phi_{(I_0)} \times \frac{(I - I_{\text{comp}})}{P_{\text{gmax}}} \right] \right\} - R_D \quad (10)$$

$$\phi_{(I)} = \frac{\phi_{(I_0)} \times P_{\text{gmax}}^3}{(\phi_{(I_0)}^2 \times I^2 + P_{\text{gmax}}^2)^{3/2}} \quad (17)$$

$$\phi_{(I)} = \phi_{(I_0)} \times \operatorname{sech}^2 \left( \frac{-\phi_{(I_0)} \times I}{P_{\text{gmax}}} \right) = \phi_{(I_0)} \times \left[ \frac{1}{\cosh^2 \left( \frac{-\phi_{(I_0)} \times I}{P_{\text{gmax}}} \right)} \right] \quad (18)$$

$$\phi_{(I)} = \frac{P_{\text{gmax}}}{I_{\text{sat}}} \times \operatorname{sech}^2 \left( \frac{I}{I_{\text{sat}}} \right) = \frac{P_{\text{gmax}}}{I_{\text{sat}}} \times \left[ \frac{1}{\cosh^2 \left( \frac{I}{I_{\text{sat}}} \right)} \right] \quad (19)$$

$$\phi_{(I)} = \frac{\phi_{(I_0)}}{2\theta} \times \left[ 1 - \frac{\phi_{(I_0)} \times I + P_{\text{gmax}} - 2\theta \times P_{\text{gmax}}}{\sqrt{(\phi_{(I_0)} \times I + P_{\text{gmax}})^2 - 4\theta \times \phi_{(I_0)} \times I \times P_{\text{gmax}}}} \right] \quad (20)$$

$$\phi_{(I)} = \phi_{(I_0)} \times \exp \left( \frac{-\phi_{(I_0)} \times I}{P_{\text{gmax}}} \right) \quad (21)$$

$$\phi_{(I)} = P_{\text{gmax}} \times k \times \exp[-k(I - I_{\text{comp}})] \quad (22)$$

$$\phi_{(I)} = \phi_{(I_0 - I_{\text{comp}})} \times \frac{1 - \beta \times \gamma \times I^2 - 2\beta \times I + (\gamma + \beta)I_{\text{comp}}}{(1 + \gamma \times I)^2} \quad (23)$$

$\phi_{(I_{\text{comp}})}$  was calculated using Eqs. 15–23, replacing  $I$  with  $I_{\text{comp}}$ .  $\phi_{(I_0 - I_{\text{comp}})}$  and  $\phi_{(I_{\text{comp}} - I_{200})}$  were calculated as the slope of the linear regression of  $P_N$  for values of  $I$  between 0 and  $I_{\text{comp}}$  and between  $I_{\text{comp}}$  and 200  $\mu\text{mol}$  (photon)  $\text{m}^{-2} \text{s}^{-1}$ , respectively.

$I_{\text{comp}}$  is one of the parameters in Eqs. 9–11. For the other equations, it was calculated by isolating  $I$  in the mathematical model and setting  $P_N$  to zero. To develop individual *Excel* routines (Eqs. 1–6, and 8) for the mathematical models employed in this study, the corresponding equations are presented in Eqs. 24–29, and 30, respectively.

$$I_{\text{comp}} = \frac{P_{\text{gmax}} \times R_D}{\phi_{(I_0)} \times (P_{\text{gmax}} - R_D)} \quad (24)$$

$$I_{\text{comp}} = \frac{I_{(50)} - R_D}{P_{\text{gmax}} - R_D} \quad (25)$$

$$I_{\text{comp}} = \frac{R_D \times P_{\text{gmax}}}{\phi_{(I_0)}} \times \sqrt{\frac{1}{P_{\text{gmax}}^2 - R_D^2}} \quad (26)$$

$$I_{\text{comp}} = \operatorname{arctanh}\left(\frac{R_D}{P_{\text{gmax}}}\right) \times \frac{P_{\text{gmax}}}{\phi_{(I_o)}} \quad (27)$$

$$I_{\text{comp}} = I_{\text{sat}} \times \operatorname{arctanh}\left(\frac{R_D}{P_{\text{gmax}}}\right) \quad (28)$$

$$I_{\text{comp}} = \frac{R_D \times (\phi_{(I_o)} \times R_D - P_{\text{gmax}})}{\phi_{(I_o)} \times (R_D - P_{\text{gmax}})} \quad (29)$$

$$I_{\text{comp}} = -\frac{P_{\text{gmax}}}{\phi_{(I_o)}} \times \left[ \ln\left(1 - \frac{R_D}{P_{\text{gmax}}}\right) \right] \quad (30)$$

$I_{(50)}$  is one of the parameters of Eq. 2, but as mentioned before, this parameter does not correspond to the desired value of  $I$ , when  $P_N$  is 50% of  $P_{\text{gmax}}$ . In this study, we decided to calculate this variable by considering it to be the value of  $I$ , when  $P_N$  is 50% of  $P_{N\text{max}}$ , which means  $0.5 (P_{\text{gmax}} - R_D)$ . To develop individual *Excel* routines

(Eqs. 1–6, 8, 9, and 11) for each of the mathematical models employed in this study, the corresponding general forms to calculate  $I_{\text{sat}(n)}$  by inserting the desired percentile value ( $n$ ) are presented in Eqs. 31–36, 37, 38, and 39, respectively.

$$I_{\text{sat}(n)} = \frac{P_{\text{gmax}} \times R_D \left(\frac{n}{100} - 1\right) - \frac{n}{100} \times P_{\text{gmax}}^2}{\phi_{(I_o)} \times \left[ P_{\text{gmax}} \left(\frac{n}{100} - 1\right) + R_D \left(1 - \frac{n}{100}\right) \right]} \quad (31)$$

$$I_{\text{sat}(n)} = \frac{I_{(50)} \times \left( R_D \times \frac{n}{100} - P_{\text{gmax}} \times \frac{n}{100} - R_D \right)}{P_{\text{gmax}} \left(\frac{n}{100} - 1\right) + R_D \left(1 - \frac{n}{100}\right)} \quad (32)$$

$$I_{\text{sat}(n)} = \frac{P_{\text{gmax}} \times \left[ \frac{n}{100} \times (P_{\text{gmax}} - R_D) + R_D \right]}{\phi_{(I_o)} \times \sqrt{P_{\text{gmax}}^2 - \left[ \frac{n}{100} \times (P_{\text{gmax}} - R_D) + R_D \right]^2}} \quad (33)$$

$$I_{\text{sat}(n)} = \operatorname{arctanh}\left[ \frac{\frac{n}{100} \times (P_{\text{gmax}} - R_D) + R_D}{P_{\text{gmax}}} \right] \times \frac{P_{\text{gmax}}}{\phi_{(I_o)}} \quad (34)$$

$$I_{\text{sat}(n)} = \operatorname{arctanh}\left[ \frac{\frac{n}{100} \times (P_{\text{gmax}} - R_D) + R_D}{P_{\text{gmax}}} \right] \times I_{\text{sat}} \quad (35)$$

$$I_{\text{sat}(n)} = \frac{P_{\text{gmax}} \left[ \frac{n}{100} \times P_{\text{gmax}} + R_D \times \left(1 - \frac{n}{100}\right) \right] - \theta \left[ \frac{n}{100} (P_{\text{gmax}} - R_D) + R_D \right]^2}{\phi_{(I_o)} \left[ P_{\text{gmax}} \left(1 - \frac{n}{100}\right) + R_D \left(\frac{n}{100} - 1\right) \right]} \quad (36)$$

$$I_{\text{sat}(n)} = \frac{P_{\text{gmax}}}{\phi_{(I_o)}} \times \left\{ -\ln \left[ 1 - \frac{\frac{n}{100} \times (P_{\text{gmax}} - R_D) + R_D}{P_{\text{gmax}}} \right] \right\} \quad (37)$$

$$I_{\text{sat}(n)} = I_{\text{comp}} - \frac{\ln \left\{ 1 - \left[ \frac{\frac{n}{100} \times (P_{\text{gmax}} - R_D)}{P_{\text{gmax}}} \right] \right\}}{k} \quad (38)$$

$$I_{\text{sat}(n)} = \frac{\left\{ \left( \phi_{(I_o - I_{\text{comp}})} \times \beta \times I_{\text{comp}} \right) - \left[ \frac{n}{100} \times (P_{\text{gmax}} - R_D) \times \gamma \right] + \phi_{(I_o - I_{\text{comp}})} \right\}}{2\phi_{(I_o - I_{\text{comp}})} \times \beta} - \sqrt{\frac{\left[ \left( \frac{n}{100} \times (P_{\text{gmax}} - R_D) \times \gamma \right) - \left( \phi_{(I_o - I_{\text{comp}})} \times \beta \times I_{\text{comp}} \right) - \phi_{(I_o - I_{\text{comp}})} \right]^2 - \left[ 4\phi_{(I_o - I_{\text{comp}})} \times \beta \times \left( \phi_{(I_o - I_{\text{comp}})} \times I_{\text{comp}} + \frac{n}{100} \times (P_{\text{gmax}} - R_D) \right) \right]}{2\phi_{(I_o - I_{\text{comp}})} \times \beta}} \quad (39)$$

Although  $I_{\text{sat}}$  is a common variable in the literature, methodological problems in its calculation detract from its intended purpose. We developed a new method to calculate this variable in the *Excel* routine, which we called  $I_{\text{max}}$  to differentiate it from  $I_{\text{sat}}$ .  $I_{\text{max}}$  is defined as the point beyond which no significant change in  $P_N$  occurs. The equipment resolution is thereby taken into account. Given a low air flow rate [ $100 \mu\text{mol}(\text{air}) \text{s}^{-1}$ ], the allowed

difference between two infrared gas analyzers for the *LI-6400* is  $0.4 \mu\text{mol}(\text{CO}_2) \text{mol}(\text{air})^{-1}$  (LI-COR 2004). Using a leaf chamber with  $6 \text{ cm}^2$ , therefore, one can calculate the maximum net photosynthetic rate that can be considered not significant multiplying the molar flow rate by the difference in the mol fraction of  $\text{CO}_2$  and dividing it by the leaf area, which gives  $0.067 \mu\text{mol}(\text{CO}_2) \text{m}^{-2} \text{s}^{-1}$ . If no significant change in  $P_N$  was found within a

50  $\mu\text{mol}(\text{photon})\text{ m}^{-2}\text{ s}^{-1}$  increment in  $I$ , we considered the previous value of  $I$  to be the exact value of  $I_{\text{max}}$ . At this point, the real light-saturated rate of net  $\text{CO}_2$  uptake ( $P_{\text{N}(I_{\text{max}})})$  was also calculated.

**The Microsoft Excel spreadsheet and the Solver function for fitting the models:** A simple routine to minimize the sum of the squares of the errors (SSE), allowing the determination of function parameters using the Solver function of *Microsoft Excel 2010*, was developed according to Brown (2001). In this case, the method employed to fit the regression curves was the least squares estimation (Ratkowsky 1983, 1990, Seber and Wild 2003), although nowadays several error analysis methods have been used to determine the best fitting equation, such as the sum of the absolute errors (SAE), average relative errors (ARE), chi-square test ( $\chi^2$ ), *etc.* (Kumar and Sivanesan 2006).

Usually, the Solver function is not automatically installed in the *Excel* program; in this case, the users must enter in the “File” main menu, go to “Options”, then “Add-Ins”, and there they can find the “Solver Add-In”. The users must choose it and then, pressing the key “Go” they are able to activate “Solver Add-In” in the proper box. Once properly activated, the “Solver” can be found in the “Data” main menu and, in this case, the users are able to start working with it.

The routine requires inputs of measurements of  $P_{\text{N}}$  and  $I$  as well as estimates of the sensitivity of the equipment used to obtain these measurements. Each of the potential fits is placed in a separate file, allowing users to choose which fits they would like to test.

The file contains two spreadsheets. The first is used to fit the regression, and it gives the goodness of fit ( $R^2$ ) as its outputs, the SSE, and all of the ecophysiological and mathematical metrics. Two graphics are also generated, showing the relationship between  $P_{\text{N}}/I$  and the overlying fit and the relationship between  $\phi$  and  $I$ . The second spreadsheet serves as a tutorial detailing how to use the Solver.

Because the fitting process is iterative, initial parameter estimates must be provided. The initial estimates and ranges used here were based on our own experience with the study of species and the literature values. However, there can be cases in which the maximum and minimum limits imposed for the parameter must be changed by the user in order to make it possible to fit the mathematical model.

The necessary primary parameters are  $P_{\text{gmax}}$ ,  $\phi_{(I_0)}$ , and  $R_{\text{D}}$ , though certain fits require additional parameters. The initial estimates for  $P_{\text{gmax}}$  can be generated using values from Nobel (1991), who compiled data from various researchers showing that the maximal rate of the net  $\text{CO}_2$  uptake for  $\text{C}_3$  species ranges from 42 to 59  $\mu\text{mol}(\text{CO}_2)\text{ m}^{-2}\text{ s}^{-1}$  and for  $\text{C}_4$  species from 57 to 75  $\mu\text{mol}(\text{CO}_2)\text{ m}^{-2}\text{ s}^{-1}$ . The initial estimates of  $R_{\text{D}}$  can be obtained as approximately 10% of the  $P_{\text{Nmax}}$ , as both parameters have a coupling relationship (Wertin and Teskey 2008).

The theoretical maximum value of the quantum yield is 0.1250  $\mu\text{mol}(\text{CO}_2)\text{ }\mu\text{mol}(\text{photon})^{-1}$  as 8 photons are required per one molecule of  $\text{CO}_2$  fixed (Luo *et al.* 2000, Singaas *et al.* 2001). However, the observed values range from 0.0266 to 0.0800  $\mu\text{mol}(\text{CO}_2)\text{ }\mu\text{mol}(\text{photon})^{-1}$ , with the change due to leaf light absorption efficiency, photorespiration, cyclic photophosphorylation, and stress factors affecting gas exchange (Singaas *et al.* 2001).

$\theta$  represents the ratio of the physical to the total resistances of  $\text{CO}_2$  diffusion, describing the sharpness of the transition from light limitation to light saturation (Jones 1988). Its theoretical range is 0 to 1, but typical values of  $\theta$  are within the range of 0.70 to 0.99 (Ögren 1993). The specific values of  $k$  in Eq. 9 range from 0.001 to 0.009  $\text{s m}^2\text{ }\mu\text{mol}(\text{photon})^{-1}$  (Prado *et al.* 1994). The value of  $I_{\text{comp}}$  varies among species, but as the first approach, we used values from 5 to 150  $\mu\text{mol}(\text{photon})\text{ m}^{-2}\text{ s}^{-1}$  that include both  $\text{C}_3$  and  $\text{C}_4$  plants. Ye (2007) did not provide any information about the ranges of  $\beta$  and  $\gamma$ . We used the range between 0 and 1 for both variables. These values provide guidance to users in choosing the proper values for parameters, but it is fundamental to take into account the data measured. Looking at the  $P_{\text{N}}/I$  pairs plotted, it is easy to identify appropriate ranges for each parameter.

When executed, the Solver function completes the iterative process necessary to fit the chosen model with all of the variables of interest previously noted. With a minimal user input, a graph of the original data with a regressed  $P_{\text{N}}/I$  curve is produced. A graph of  $\phi$  as a function of  $I$  is produced automatically.

To determine the best fit to the data, all of the model forms should be tested and compared *via* SSE. The best model presents the lowest SSE. We do not recommend the use of  $R^2$  for model selection, as  $R^2$  has no obvious meaning for nonlinear regression and it is not employed for this purpose (Ratkowsky 1983, 1990).

#### **Estimating population means and confidence intervals for the regression parameters and the measured variables:**

The measurement of the original  $P_{\text{N}}/I$  data pairs is performed for each individual sample, so each leaf has its own  $P_{\text{N}}/I$  curve to be fitted. In this case, a single mathematical model is often (but not necessarily always) employed for all the replicates. It is also possible that intrinsic natural variations lead to differences between samples of the same population, which necessitates different mathematical models to be applied for specific cases. As previously mentioned, in each case, the method for choosing the best model is to identify the model showing the minimum SSE.

Once all the replicates were evaluated, it is necessary to characterize the population by obtaining the mean value and a confidence interval for each regression parameter or measured variable. As the aim of this manuscript was only to present the tools for researchers and students to fit the best  $P_{\text{N}}/I$  curve, we used only a single sample

and did not work with replicates. To deal with it, we recommend the method of resampling with replacement, using at least 1000 resamplings. It is easy to develop an

## Results and discussion

The aim of this work was to present the most common models used for  $P_N/I$  curves fitted by the Solver function of *Microsoft Excel*. The results are widely accessible and didactically useful, showing the computation of all of the regression parameters and calculated variables. Users can now compute both  $P_N/C_c$  curves according to the procedure explained by Sharkey *et al.* (2007), and  $P_N/I$  curves according to the procedure explained in this manuscript, using the same package, effectively presenting the biochemical and photochemical efficiency and capacity of the photosynthetic process.

In our opinion, there is no single definitive mathematical model to describe the  $P_N/I$  curve that should be employed in all situations. Several researchers have been developing mathematical models to fit  $P_N/I$  curves, and year after year, they found something, which was not taken into account at that moment, and then they presented a new mathematical model with that novelty. In

*Excel* routine to perform this calculation for each variable, deriving the mean and confidence intervals following the step-by-step procedure detailed by Christie (2004).

our opinion, all of these improvements are welcome, but they must be considered very carefully because of their specificity, which renders very often any generalization impossible. From this perspective, the best  $P_N/I$  curve is the one among all available that fits best the original data.

In this study of *V. divergens*, the mathematical model, which fitted the best the original data of  $P_N/I$  curve, was the nonrectangular hyperbola (Eq. 6). This model was chosen because it had the lowest SSE (Fig. 1F). All of the regression parameters of the models employed are presented in Table 2.

Models based on the same principle are quite similar and in dependence on the original data they can provide solutions with high or low equality, and even precisely the same value. In this case, one could see that Eqs. 1 and 2, based on the Michaelis-Menten model (Fig. 1A,B), Eqs. 4 and 5, based on a hyperbolic tangent model (Fig. 1D,E), and Eqs. 8 and 9, based on an exponential model

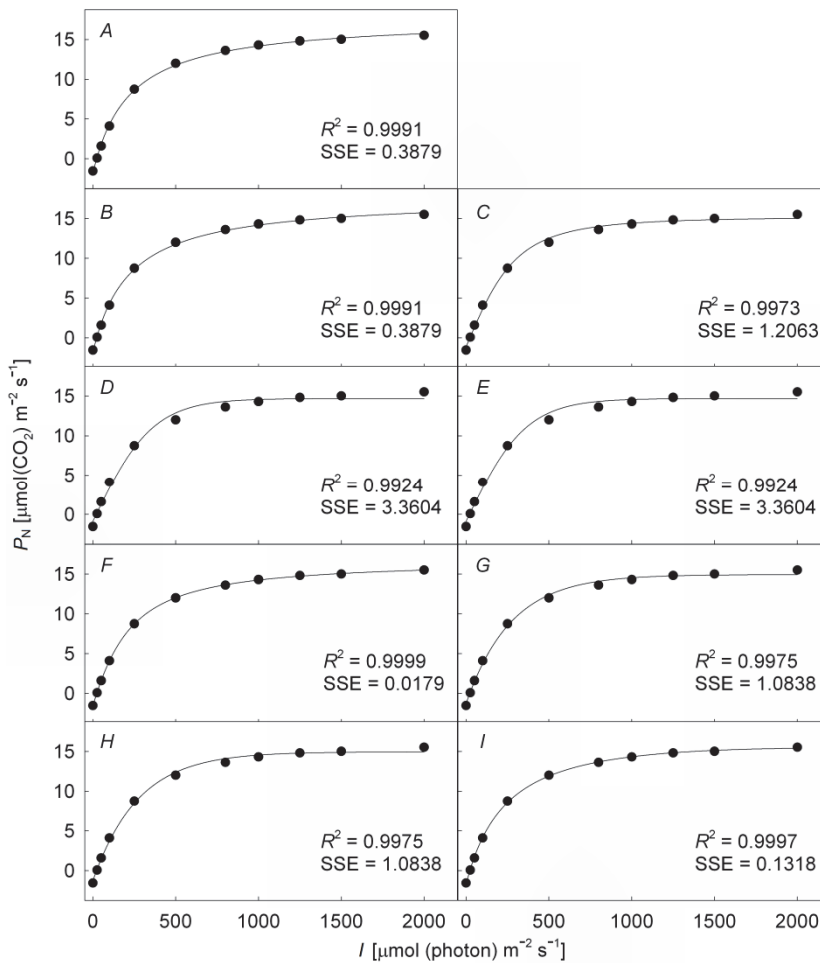


Fig. 1. Fitting  $P_N/I$  curves by applying different mathematical models for *V. divergens*. The models represented by the Eqs. 1–6, 8, 9, and 11 are represented by the regression lines in A–F, G, H, and I, respectively.  $P_N$  – net photosynthetic rate;  $I$  – photosynthetic photon flux density.

Table 2. The parameters of the regression models employed to fit the net photosynthetic light response curves of *V. divergens*.  $I_{\text{comp}}$  – light compensation point [ $\mu\text{mol}(\text{photon}) \text{m}^{-2} \text{s}^{-1}$ ];  $I_{\text{sat}}$  – light saturation point [ $\mu\text{mol}(\text{photon}) \text{m}^{-2} \text{s}^{-1}$ ];  $I_{(50)}$  – light saturation point for  $P_{\text{N}} + R_{\text{D}}$  equal to 50% of  $P_{\text{Nmax}}$  [ $\mu\text{mol}(\text{photon}) \text{m}^{-2} \text{s}^{-1}$ ];  $k$  – adjusting factor [ $\text{s m}^2 \mu\text{mol}(\text{photon})^{-1}$ ];  $P_{\text{gmax}}$  – maximum gross photosynthetic rate [ $\mu\text{mol}(\text{CO}_2) \text{m}^{-2} \text{s}^{-1}$ ];  $R_{\text{D}}$  – dark respiration [ $\mu\text{mol}(\text{CO}_2) \text{m}^{-2} \text{s}^{-1}$ ];  $\beta$  – adjusting factor (dimensionless);  $\gamma$  – adjusting factor (dimensionless);  $\theta$  – convexity factor (dimensionless);  $\phi_{(I_0)}$  – quantum yield at  $I = 0 \mu\text{mol}(\text{photon}) \text{m}^{-2} \text{s}^{-1}$  [ $\mu\text{mol}(\text{CO}_2) \mu\text{mol}(\text{photon})^{-1}$ ];  $\phi_{(I_0 - I_{\text{comp}})}$  – quantum yield at the range between  $I = 0 \mu\text{mol}(\text{photon}) \text{m}^{-2} \text{s}^{-1}$  and  $I_{\text{comp}}$  [ $\mu\text{mol}(\text{CO}_2) \mu\text{mol}(\text{photon})^{-1}$ ].

| Parameters                       | Mathematical models |       |        |        |       |        |        |        |        |
|----------------------------------|---------------------|-------|--------|--------|-------|--------|--------|--------|--------|
|                                  | Eq. 1               | Eq. 2 | Eq. 3  | Eq. 4  | Eq. 5 | Eq. 6  | Eq. 8  | Eq. 9  | Eq. 11 |
| $P_{\text{gmax}}$                | 19.5                | 19.5  | 16.4   | 15.5   | 15.5  | 18.4   | 16.2   | 15.6   |        |
| $\phi_{(I_0)}$                   | 0.0899              |       | 0.0493 | 0.0433 |       | 0.0709 | 0.0597 |        |        |
| $\phi_{(I_0 - I_{\text{comp}})}$ |                     |       |        |        |       |        |        |        | 0.0756 |
| $R_{\text{D}}$                   | 1.8                 | 1.8   | 1.1    | 0.9    | 0.9   | 1.6    | 1.3    | 0.6    |        |
| $I_{\text{sat}}$                 |                     |       |        |        | 359.2 |        |        |        |        |
| $I_{(50)}$                       |                     | 216.4 |        |        |       |        |        |        |        |
| $\theta$                         |                     |       |        |        |       | 0.4325 |        |        |        |
| $K$                              |                     |       |        |        |       |        |        | 0.0037 |        |
| $I_{\text{comp}}$                |                     |       |        |        |       |        |        | 10.5   | 22.6   |
| $\beta$                          |                     |       |        |        |       |        |        |        | 4.3E-5 |
| $\gamma$                         |                     |       |        |        |       |        |        |        | 0.0039 |

Table 3. The variables calculated from the models.  $I_{\text{comp}}$  – light compensation point [ $\mu\text{mol}(\text{photon}) \text{m}^{-2} \text{s}^{-1}$ ];  $I_{\text{max}}$  – light saturation point beyond which there is no significant change in  $P_{\text{N}}$  [ $\mu\text{mol}(\text{photon}) \text{m}^{-2} \text{s}^{-1}$ ];  $I_{\text{sat}}$  – light saturation point [ $\mu\text{mol}(\text{photon}) \text{m}^{-2} \text{s}^{-1}$ ];  $I_{\text{sat}(50)}$  – light saturation point for  $P_{\text{N}} + R_{\text{D}}$  equal to 50% of  $P_{\text{Nmax}}$  [ $\mu\text{mol}(\text{photon}) \text{m}^{-2} \text{s}^{-1}$ ];  $I_{\text{sat}(85)}$  – light saturation point for  $P_{\text{N}} + R_{\text{D}}$  equal to 85% of  $P_{\text{Nmax}}$  [ $\mu\text{mol}(\text{photon}) \text{m}^{-2} \text{s}^{-1}$ ];  $I_{\text{sat}(90)}$  – light saturation point for  $A + R_{\text{D}}$  equal to 90% of  $P_{\text{Nmax}}$  [ $\mu\text{mol}(\text{photon}) \text{m}^{-2} \text{s}^{-1}$ ];  $I_{\text{sat}(95)}$  light saturation point for  $P_{\text{N}} + R_{\text{D}}$  equal to 95% of  $P_{\text{Nmax}}$  [ $\mu\text{mol}(\text{photon}) \text{m}^{-2} \text{s}^{-1}$ ];  $P_{\text{gmax}}$  – maximum gross photosynthetic rate [ $\mu\text{mol}(\text{CO}_2) \text{m}^{-2} \text{s}^{-1}$ ];  $P_{\text{N}(I_{\text{max}})}$  – maximum net photosynthetic rate obtained at  $I = I_{\text{max}}$  [ $\mu\text{mol}(\text{CO}_2) \text{m}^{-2} \text{s}^{-1}$ ];  $R_{\text{D}}$  – dark respiration [ $\mu\text{mol}(\text{CO}_2) \text{m}^{-2} \text{s}^{-1}$ ];  $\phi_{(I_{\text{comp}})}$  – quantum yield at  $I = I_{\text{comp}}$  [ $\mu\text{mol}(\text{CO}_2) \mu\text{mol}(\text{photon})^{-1}$ ];  $\phi_{(I_{\text{comp}} - I_{200})}$  – quantum yield at the range between  $I_{\text{comp}}$  and  $I = 200 \mu\text{mol}(\text{photon}) \text{m}^{-2} \text{s}^{-1}$  [ $\mu\text{mol}(\text{CO}_2) \mu\text{mol}(\text{photon})^{-1}$ ];  $\phi_{(I_0)}$  – quantum yield at  $I = 0 \mu\text{mol}(\text{photon}) \text{m}^{-2} \text{s}^{-1}$  [ $\mu\text{mol}(\text{CO}_2) \mu\text{mol}(\text{photon})^{-1}$ ];  $\phi_{(I_0 - I_{\text{comp}})}$  – quantum yield at the range between  $I = 0 \mu\text{mol}(\text{photon}) \text{m}^{-2} \text{s}^{-1}$  and  $I_{\text{comp}}$  [ $\mu\text{mol}(\text{CO}_2) \mu\text{mol}(\text{photon})^{-1}$ ]. \*Photosynthetic active radiation values above the range employed to make the measurements. \*\*Photosynthetic active radiation values above the maximum that reaches the Earth’s surface.

| Calculated variables                 | Mathematical models |           |         |        |        |           |         |         |          |
|--------------------------------------|---------------------|-----------|---------|--------|--------|-----------|---------|---------|----------|
|                                      | Eq. 1               | Eq. 2     | Eq. 3   | Eq. 4  | Eq. 5  | Eq. 6     | Eq. 8   | Eq. 9   | Eq. 11   |
| $I_{\text{comp}}$                    | 22.5                | 22.5      | 22.7    | 20.2   | 20.2   | 23.4      | 22.0    |         |          |
| $I_{\text{sat}(50)}$                 | 261.4               | 261.4     | 209.4   | 211.0  | 211.0  | 235.6     | 210.1   | 187.6   | 211.1    |
| $I_{\text{sat}(85)}$                 | 1,376.3             | 1,376.3   | 559.2   | 462.4  | 462.4  | 1,022.7   | 537.0   | 468.1   | 678.0    |
| $I_{\text{sat}(90)}$                 | 2,172.6*            | 2,172.6*  | 713.1   | 539.8  | 539.8  | 1,564.3   | 647.0   | 549.4   | 854.6    |
| $I_{\text{sat}(95)}$                 | 4,561.7**           | 4,561.7** | 1,047.6 | 668.7  | 668.7  | 3,179.1** | 835.2   | 665.9   | 1,148.4  |
| $I_{\text{sat}}$                     |                     |           |         |        |        |           |         |         | 2,289.9* |
| $I_{\text{max}}$                     | 1537.0              | 1,949.0   | 1,030.0 | 847.0  | 847.0  | 1,348.0   | 1,008.0 | 1,008.0 | 1,297.0  |
| $P_{\text{gmax}}$                    |                     |           |         |        |        |           |         |         | 17.1     |
| $P_{\text{N}(I_{\text{max}})}$       | 15.2                | 15.7      | 14.5    | 14.4   | 14.4   | 14.9      | 14.5    | 14.5    | 14.9     |
| $R_{\text{D}}$                       |                     |           |         |        |        |           |         |         | 1.7      |
| $\phi_{(I_0)}$                       |                     | 0.0899    |         |        |        | 0.0433    |         | 0.0597  | 0.0824   |
| $\phi_{(I_{\text{comp}})}$           | 0.0738              | 0.0738    | 0.0490  | 0.0431 | 0.0431 | 0.0638    | 0.0550  | 0.0574  | 0.0694   |
| $\phi_{(I_0 - I_{\text{comp}})}$     | 0.0816              | 0.0816    | 0.0492  | 0.0432 | 0.0432 | 0.0674    | 0.0573  | 0.0586  | 0.0757   |
| $\phi_{(I_{\text{comp}} - I_{200})}$ | 0.0410              | 0.0410    | 0.0416  | 0.0391 | 0.0391 | 0.0421    | 0.0400  | 0.0410  | 0.0409   |

(Fig. 1G,H) provided quite similar or even identical results; therefore, they had almost the same values for their regression parameters (Table 2), and the variables calculated from those models were approximately of the

same magnitude (Table 3).

There is a difference between what is expected from the maximum theoretical velocity ( $V_{\text{max}}$ ) for an enzyme and  $P_{\text{gmax}}$ . If we remember that  $V_{\text{max}}$  is a constant for a



given enzyme that is achieved, when all of the enzyme molecules have tightly bound their substrate, but that this rate of enzymatic activity is never actually achieved, then for all of the mathematical models, in which  $P_{gmax}$  is an asymptote reached at infinite  $I$ , there is no doubt that  $P_{gmax}$  has exactly the same connotation. In those cases,  $P_{gmax}$  can not be employed as an explanatory variable to define the maximum photosynthetic capacity of species, because it does not exist in real life. In this case, our proposition to employ  $P_{N(I_{max})}$  instead of  $P_{gmax}$  is justified by the fact that the primer is always found in the range of the measured data and it exactly represents the highest value of  $P_N$  to be achieved by that species in the experimental conditions to which it was subjected. This argument has to be taken into account, particularly because there is also an ecophysiological interest in knowing at which value of  $I$  the value of  $P_{N(I_{max})}$  can be achieved. Because for  $P_{gmax}$  the natural value of  $I$  is infinite by definition, several authors proposed the use of  $I_{sat(n)}$ , which is taken to be the corresponding value of light, when  $P_N$  reaches a percentile of  $P_{Nmax}$ , which leads to the same inadequacy. Independent of which fraction is taken into account, it is not reasonable to use  $I_{sat(n)}$  as an ecophysiological indicator of the maximum light that saturates  $P_N$ , because it does not represent the desired concept.

The maximum instantaneous value of the solar irradiance perpendicularly incident on the Earth's atmosphere, which is known as the solar constant ( $S$ ), is  $1,366 \pm 46 \text{ W m}^{-2}$  (Jones *et al.* 2003, Nobel 2009). Because of atmospheric attenuation, on the clearest days, the maximum value of the solar irradiance that reaches the Earth's surface can be approximately 75% of  $S$  (Campbell and Norman 1998). Because the maximum value of  $I$  is approximately 50% of the fraction of  $S$  that reaches the Earth's surface (Stanhill and Fuchs 1977, Jacovides *et al.* 2003), the maximum value of  $I$  is  $530 \text{ W m}^{-2}$ . By converting this radiometric unit to a photometric unit and considering a wavelength of 550 nm to be representative of the photosynthetic active radiation (Campbell and Norman 1998, Jones *et al.* 2003), the maximum value of  $I$  is  $2,435 \mu\text{mol}(\text{photon}) \text{ m}^{-2} \text{ s}^{-1}$  or slightly higher, due to the diffuse radiation that can enhance this value. Clearly, the values of  $I_{sat}$  above this maximum limit have no realistic ecophysiological meaning.

Several researchers adopt a value of  $I_{sat}$ , in which  $P_N$  is equal to 50% ( $I_{sat(50)}$ ), 90% ( $I_{sat(90)}$ ), or 95% ( $I_{sat(95)}$ ) of the  $P_{gmax}$ , to overcome the fact that  $P_{gmax}$  is an asymptote, a value, in which  $I$  is infinite. When this method is used, not only  $P_{gmax}$  but also  $I_{sat(n)}$  is a forced representation of the reality.

Kaipiainen (2009) uses a modified Michaelis-Menten model (Eq. 2) to estimate  $I_{(50)}$ , which does not have the same meaning as  $I_{sat(50)}$ , because, as we noted before,  $I_{(50)}$  is the value of  $I$ , when  $P_N + R_D = 0.5 P_{gmax}$ , and  $I_{sat(50)}$  is the value of  $I$ , when  $P_N = 0.5 (P_{gmax} - R_D)$ . However, Kaipiainen (2009) considers that despite the fraction of

$P_{gmax}$  that is taken, those different values of  $I$  obtained, when  $P_N + R_D = 50, 90,$  or  $95\%$  of  $P_{gmax}$ , have "similar physiological meaning". We disagree with this statement, because if applying our approach (Eq. 32),  $I_{sat(90)}$  and  $I_{sat(95)}$  (Table 3) were 731 and 1,645% higher, respectively, than  $I_{sat(50)}$  (Table 3). Obviously, these estimates cannot be considered to be similar in terms of plant ecophysiology. In addition, as one can see from Table 3, the estimates of  $I_{sat(90)}$  derived from Eqs. 1 and 2 were out of the range employed to obtain the measurements, and the  $I_{sat(95)}$  estimates derived from Eqs. 1, 2, and 6 were higher than the maximum theoretical value that can reach Earth's surface.

The modified rectangular hyperbola model (Eq. 11) proposed by Ye (2007) to solve this problem gave a reasonable value of  $P_{gmax}$  (Table 2). However, the magnitude of  $I_{sat}$  achieved (Table 3) using Eq. 14 was out of the range of the original data measured.

We suggest that  $P_{N(I_{max})}$  is a better variable to represent realistically the maximum net photosynthetic rate beyond which no significant increment can be achieved with an additional increment in  $I$ , and  $I_{max}$  is exactly that point at which  $P_{N(I_{max})}$  is found. These variables are much more appropriate for the representation of the photosynthetic capacity than any other variables proposed to date. Their interpretation is immediate and obvious, and their magnitude is always in the range, in which the measurements were performed.

Fig. 2 displays the results obtained for  $\phi_{(I)}$  from each model; the results served as an important reminder to select the most appropriate model. For example, model estimates of  $\phi_{(I)}$  that vary by 100% can be observed, especially at low  $I$ . The only way to be closer to the best approach of  $\phi_{(I)}$  or any other variable taken from the mathematical model is by choosing the best fitted model. Because  $R^2$  for nonlinear models cannot fulfill this expectation (Ratkowsky 1983, 1990), the best model can be achieved by choosing that with the minimal value of SSE. Fitting the best model provides the best approximation of reality; therefore, the search for the best model becomes crucial for interpreting all of the information, which the model can offer as correctly as possible.

Another important comment must be given with respect to quantum yield in Eqs. 1, 3, 4, 6–8, and 10 in which it appears as  $\phi_{(I_0)}$ , and in Eq. 11, in which it appears as  $\phi_{(I_0 - I_{comp})}$ . In all of these cases,  $\phi_{(I_0)}$  and  $\phi_{(I_0 - I_{comp})}$  do not correspond with the original concept of this parameter, which tells us that the quantum yield (actually  $\phi_{(I_{comp} - I_{200})}$ , in our terminology) is the slope of the curve at its linear portion in the range of approx.  $I = I_{comp}$  to  $I = 200 \mu\text{mol}(\text{photon}) \text{ m}^{-2} \text{ s}^{-1}$ , representing the "maximum quantum yield".

First of all, it is important to realize that  $\phi_{(I_0)}$  is the derivative of the model at  $I$  equals to zero. In this case, it is obtained at darkness, when no photosynthesis is possible.

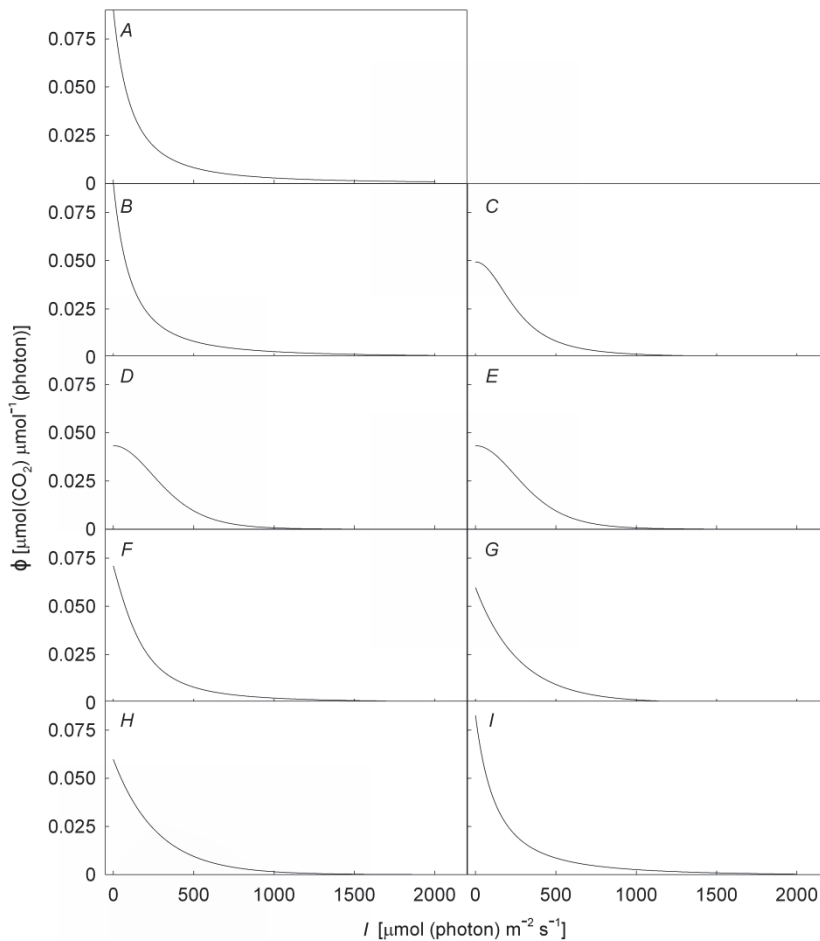


Fig. 2. The quantum yield as a function of light in *V. divergens*. The models represented by the derivative Eqs. 15–23 are represented by the curves in A–I, respectively.  $I$  – photosynthetic photon flux density;  $\phi$  – quantum yield.

In this case, this variable cannot explain the “maximum quantum yield”. Second, there is not a “linear portion” in that curvilinear model in its *stricto sensu*, and that shape is not due to a model that cannot correctly fit the data in that portion but arises, because the curvilinear shape is exactly how  $P_N$  changes with  $I$  in most cases. In fact, forcing any straight line in any portion of the curve could be unrealistic and arbitrary. In this case, it was obvious that  $\phi_{(I_0)}$  is always the maximum value of the quantum yield, higher than any other point at the  $P_N/I$  curve. However,  $\phi_{(I_0)}$  has no realistic meaning in terms of plant ecophysiology, because no positive net assimilation is possible in complete darkness.

The original definition of the quantum yield is “the ratio of the moles of product formed or substrate consumed to the moles of photons absorbed”, the maximum quantum yield is defined as “the largest quantity of product formed or substrate consumed to the smallest number of photons absorbed” (Falkowski and Raven 2007). However, it is important to note that the relationship between the absorbed light and the  $O_2$  evolution can be different from the relationship between the absorbed light and the  $CO_2$  uptake or net  $CO_2$  uptake. For ecophysiological purposes, the maximum  $\phi$  appears to be better represented as the ratio of the net  $CO_2$  evolution to

the absorbed (or incident) light in the region of the  $P_N/I$  curve, where positive  $CO_2$  assimilation begins. We prefer the approach adopted by Ye (2007), which describes the variation in  $\phi_{(I)}$  with a progressive increase of  $I$ , which has an obvious decreasing tendency (Fig. 2). Additionally, we prefer to use the term “apparent quantum yield”, when the light employed is not that absorbed by the leaf, but instead, the incident light, and no correction to eliminate the effect of photorespiration is performed as recommended to access the real “maximum quantum yield” (Long and Hällgren 1993, Singaas *et al.* 2001).

In their critiques of different methods to calculate the quantum yield and the discrepancy between the published values, Singaas *et al.* (2001) noted something that we have already mentioned about using  $O_2$  evolution or  $CO_2$  assimilation methods, which represent different moments in the process of photosynthesis. They also comment that to identify the correct maximum quantum yield, which they stated, must be the nearest to the theoretical value of 0.125, it is important to use the absorbed, not incident  $I$  values and to identify the linear portion of the  $P_N/I$  curve correctly, which can be accomplished by eliminating photorespiration at low  $O_2$  keeping the intercellular  $CO_2$  concentration ( $C_i$ ) constant or correcting it mathematically. In our opinion, there are several questions that

must be considered in this context. As we stated in the previous paragraph, the most common shape of the  $P_N/I$  curve is curvilinear throughout its length, thus, no linear phase is clearly identifiable. However, if the shape is very close to linear, the method that Singsaas *et al.* (2001) employed to determine how much of the data could be included in that phase is inappropriate. As mentioned by Dubois *et al.* (2007), the upward progression in the coefficient of determination ( $R^2$ ) with the withdrawal of observations is inherent to its definition, thus, this parameter cannot be used as a criterion to choose data to be included or excluded from the estimation. Depending on the focus, in terms of ecophysiological research, it appears to be much more reasonable to use one theoretical maximum quantum yield ( $\phi_{\max} = 0.125$ ) as the reference to identify how stress factors or specific treatments applied to the plant can affect quantum yield or any other  $P_N/I$  parameter or calculated variable.

For us, the approach of Ye (2007) to calculation of  $\phi_{(I)}$  produces a result that is much more realistic and useful, because one can observe how the variable can change with  $I$ , and particularly for ecophysiological purposes, all of those points in the curve can be analyzed, when  $P_N$  is above the light compensation point, which means that a net  $\text{CO}_2$  uptake is taking place. The variables  $\phi_{(I_0)}$ ,

$\phi_{(I_0 - I_{\text{comp}})}$ , and  $\phi_{(I_{\text{comp}})}$  all fail in representing the maximum value of the quantum yield, because they are defined below or at the light compensation point.  $\phi_{(I_{\text{comp}} - I_{200})}$  is also problematic in fixing the point at which the calculation of the quantum yield must be performed, and depending on the species. Thus, this value may not be reasonable.

By applying the approach of Ye (2007), the values of quantum yield can be analyzed not only, when  $P_N$  is dependent on  $I$ , but also when  $P_N$  becomes progressively independent of  $I$ . This capability is very useful for evaluating differences in the photosynthetic efficiency between sun and shade leaves, for which, not always but frequently, no difference in  $\phi$  can be observed in the initial portion of the  $P_N/I$  curve.

In conclusion, we consider that our *Excel* routines are an interesting alternative for users with any level of statistical knowledge to evaluate and quickly identify the best model of  $P_N/I$  curve that fits better their experimental data. We also consider that the variables, which better represent the light-saturated rate of  $\text{CO}_2$  uptake, the light saturation point, and the quantum yield are  $P_{N(I_{\max})}$ ,  $I_{\max}$ , and  $\phi_{(I)}$ , respectively.

## References

- Abe, M., Yokota, K., Kurashima, A., Maegawa, M.: High water temperature tolerance in photosynthetic activity of *Zostera japonica* Ascherson and Graebner seedlings from Ago Bay, Mio Prefecture, central Japan. – *Fish. Sci.* **75**: 1117-1123, 2009.
- Baly, E.C.C.: The kinetics of photosynthesis. – *Proc. R. Soc. Lond. B* **117**: 218-239, 1935.
- Brown, A.M.: A step-by-step guide to non-linear regression analysis of experimental data using a Microsoft Excel spreadsheet. – *Comput. Methods Programs Biomed.* **65**: 191-200, 2001.
- Campbell, G.S., Norman, J.M.: *An Introduction to Environmental Biophysics*. 2<sup>nd</sup> Ed. Springer-Verlag, New York 1998.
- Chen, L., Tam, N.F.Y., Huang, J. *et al.*: Comparison of ecophysiological characteristics between introduced and indigenous mangrove species in China. – *Est. Coast Shelf Sci.* **79**: 644-652, 2008.
- Christie, D.: Resampling with Excel. – *Teach. Stat.* **26**: 9-13, 2004.
- Devacht, S., Lootens, P., Roldán-Ruiz, I. *et al.*: Influence of low temperatures on the growth and photosynthetic activity of industrial chicory, *Cichorium intybus* L. partim. – *Photosynthetica* **47**: 372-380, 2009.
- Donovan, T.M., Welden, C.W.: *Spreadsheet Exercises in Ecology and Evolution*. Sinauer Associates, Sunderland 2002.
- Dubois, J.-J.B., Fiscus, E.L., Booker, F.L. *et al.*: Optimizing the statistical estimation of the parameters of the Farquhar-Von Caemmerer-Berry model of photosynthesis. – *New Phytol.* **176**: 402-414, 2007.
- Falkowski, P.G., Raven, J.A.: *Aquatic Photosynthesis*. Princeton University Press, Princeton 2007.
- Gallegos, C.L., Platt, T.: Photosynthesis measurements on natural populations of phytoplankton: numerical analysis. – *Can. Bull. Fish. Aquat. Sci.* **210**: 103-112, 1981.
- Govindjee, Beatty, J.T., Gest, H., Allen, J.F.: *Discoveries in Photosynthesis*. Springer, Dordrecht 2005.
- Harley, P.C., Baldocchi, D.D.: Scaling carbon dioxide and water vapor exchange from leaf to canopy in a deciduous forest. I. Leaf model and parametrization. – *Plant Cell Environ.* **18**: 1146-1156, 1995.
- Hunt, R., Causton, D.R., Shipley, B., Askew, A.P.: A modern tool for classical growth analysis. – *Ann. Bot.* **90**: 485-488, 2002.
- Jacovides, C.P., Tymvios, F.S., Asimakopoulos, D.N. *et al.*: Global photosynthetically active radiation and its relationship with global solar radiation in the Eastern Mediterranean basin. – *Theor. Appl. Climatol.* **74**: 227-233, 2003.
- Jassby, A.D., Platt, T.: Mathematical formulation of the relationship between photosynthesis and light for phytoplankton. – *Limnol. Oceanogr.* **21**: 540-547, 1976.
- Jones, H.B., Archer, N., Rotenberg, E., Casa, R.: Radiation measurement for plant ecophysiology. – *J. Exp. Bot.* **54**: 879-889, 2003.
- Jones, M.B.: Photosynthetic responses of  $\text{C}_3$  and  $\text{C}_4$  wetland species in a tropical swamp. – *J. Ecol.* **76**: 253-262, 1988.
- Kaipainen, E.L.: Parameters of photosynthesis light curve in *Salix dasyclados* and their changes during the growth season. – *Russ. J. Plant Physiol.* **56**: 445-453, 2009.
- Kok, B.: On the interrelation of respiration and photosynthesis in green plants. – *Biochim. Biophys. Acta* **3**: 625-631, 1949.

- Kumar, K.V., Sivanesan, S.: Isotherm parameters for basic dyes onto activated carbon: comparison of linear and non-linear method. – *J. Hazard. Mater.* **129**: 147-150, 2006.
- Lambers, H., Chapin III, F.S., Pons, T.L.: Response of photosynthesis to light. – In: Lambers, H., Chapin III, F.S., Pons, T.L. (eds.): *Plant Physiological Ecology*. Pp. 26-47. Springer, New York 2008.
- LI-COR Bioscience: Using the LI-6400 Version 5. LI-COR Bioscience, Inc., Lincoln, NE, USA 2004.
- Lloyd, J., Grace, C., Miranda, A.C. *et al.*: A simple calibrated model of Amazon rainforest productivity based on leaf biochemical properties. – *Plant Cell. Environ.* **18**: 1129-1145, 1995.
- Long, S.P., Hällgren, J.-E.: Measurement of CO<sub>2</sub> assimilation by plants in the field and the laboratory. – In: Hall, D.O., Scurlock, J.M.O., Bolhär-Nordenkampf, H.R. *et al.* (eds.): *Photosynthesis and Production in a Changing Environment. A Field and Laboratory Manual*. Pp. 129-167. Chapman and Hall, London 1993.
- Lootens, P., Van Waes, J., Carlier, L.: Effect of a short photo-inhibition stress on photosynthesis, chlorophyll *a* fluorescence and pigment contents of different maize cultivars. Can a rapid and objective stress indicator be found? – *Photosynthetica* **42**: 187-192, 2004.
- Luo, Y., Hui, D., Cheng, W. *et al.*: Canopy quantum yield in a mesocosm study. – *Agric. For. Meteorol.* **100**: 35-48, 2000.
- Nobel, P.S.: *Physicochemical and Environmental Plant Physiology*. Elsevier, Amsterdam 2009.
- Nobel, P.S.: Achievable productivities of certain CAM plants: basis for high values compared with C<sub>3</sub> and C<sub>4</sub> plants. – *New Phytol.* **119**: 183-205, 1991.
- Ögren, E.: Convexity of the photosynthetic light-response curve in relation to intensity and direction of light during growth. – *Plant Physiol.* **101**: 1013-1019, 1993.
- Prado, C.H.B.A., de Moraes, J.P.A.P.V., de Mattos, E.A.: Gas exchange and leaf water status in potted plants of *Copaifera langsdorffii*. 1. Responses to water stress. – *Photosynthetica* **30**: 207-213, 1994.
- Prado, C.H.B.A., de Moraes, J.P.A.P.V.: Photosynthetic capacity and specific leaf mass in twenty woody species of cerrado vegetation under field conditions. – *Photosynthetica* **33**: 103-112, 1997.
- Prioul, J.L., Chartier, P.: Partitioning of transfer and carboxylation components of intracellular resistance to photosynthetic CO<sub>2</sub> fixation: A critical analysis of the methods used. – *Ann. Bot.* **41**: 789-800, 1977.
- Ratkowsky, D.A.: *Nonlinear Regression Modeling – A Unified Practical Approach*. Marcel Dekker, New York 1983.
- Ratkowsky, D.A.: *Handbook of Nonlinear Regression Models*. Marcel Dekker, New York 1990.
- Seber, G.A.F., Wild, C.J.: *Nonlinear Regression*. Wiley-Interscience, Hoboken 2003.
- Sharkey, T.D., Bernacchi, C.J., Farquhar, G.D., Singaas, E.L.: In Practice: Fitting photosynthetic carbon dioxide response curves for C<sub>3</sub> leaves. – *Plant Cell Environ.* **30**: 1035-1040, 2007.
- Singaas, E.L., Ort, D.R., DeLucia, E.H.: Variation in measured values of photosynthetic quantum yield in ecophysiological studies. – *Oecologia* **128**: 15-23, 2001.
- Smith, E.L.: Photosynthesis in relation to light and carbon dioxide. – *PNAS* **22**: 504-511, 1936.
- Stanhill, G., Fuchs, M.: The relative flux density of photosynthetically active radiation. – *J. Appl. Ecol.* **14**: 317-322, 1977.
- Vervuren, P.J.A., Beurskens, M.H.H., Blom, C.W.P.M.: Light acclimation, CO<sub>2</sub> response and long-term capacity of underwater photosynthesis in three terrestrial plant species. – *Plant Cell Environ.* **22**: 959-968, 1999.
- Webb, W.L., Newton, M., Starr, D.: Carbon dioxide exchange of *Alnus rubra*: a mathematical model. – *Oecologia* **17**: 281-291, 1974.
- Wertin, T.M., Teskey, R.O.: Close coupling of whole-plant respiration to net photosynthesis and carbohydrates. – *Tree Physiol.* **28**: 1831-1840, 2008.
- Ye, Z.-P.: A new model for relationship between irradiance and the rate of photosynthesis in *Oryza sativa*. – *Photosynthetica* **45**: 637-640, 2007.
- Zeinalov, Y.: Mechanisms of photosynthetic oxygen evolution and fundamental hypotheses of photosynthesis. – In: Pessaraki, M. (ed.): *Handbook of Photosynthesis*. Pp. 3-19. Taylor and Francis, Boca Ratón 2005.